

2014

# BioTechnology

*An Indian Journal*

FULL PAPER

BTAIJ, 10(23), 2014 [14540-14548]

## Dynamics of a two-degree-of freedom system with a rigid stop: Chattering-impact and subharmonic motions

Xifeng Zhu

School of Mechatronic Engineering, Lanzhou Jiaotong University, Lanzhou, 730070,  
(P.R.CHINA)

E-mail: zhuxf@mail.lzjtu.cn

### ABSTRACT

The dynamic model of a two-degree-of-freedom system with a rigid stop is considered. The multi-impact motions of the one excitation period, subharmonic motions and chattering-impact characteristics of the system are analyzed by Runge-Kutta numerical simulation algorithm, and furthermore the saddle-node and grazing bifurcations between  $p/1$  motions are revealed exactly. The research results show that a series of grazing bifurcations occur with decreasing frequency so that the impact number  $p$  of  $p/1$  motions correspondingly increases one by one, a series of saddle-node bifurcations occur with increasing frequency so that the impact number  $p$  of  $p/1$  motions correspondingly decreases one by one and there exists frequency hysteresis range and multiple coexistence attractors between  $p/1$  and  $(p+1)/1$  motions. In the low exciting frequency case, the impact number  $p$  of  $p/1$  motions becomes big enough and chattering-impact characteristics will be appearing. The transition law from  $1/1$  motion to chattering-impact motion is summarized explicitly.

### KEYWORDS

Vibration; Chattering-impact; Subharmonic motion; Bifurcation; Coexistence attractors.



INTRODUCTION

The rigid stop that can display rich and complex nonlinear responses exists extensively in mechanical vibro-impact systems. Such non-smooth nonlinear systems are capable of exhibiting classically nonlinear behaviour such as coexistence attractors, period-doubling and grazing bifurcations. For example, impact dampers, pile drivers, etc., is based on the impact action for moving bodies. With other equipment, e.g., mechanisms with clearances and barriers, gears, wheel-rail interaction of railway coaches, etc., impacts also occur, but they are detrimental as they bring about increased wear and impulsive noise. It is necessary to be able accurately to model the dynamics of mechanical systems with rigid stops and clearances, so as to enlarge profitable effects and weaken adverse effects. The near-grazing impacting behaviours such as multi-periodic orbits, subharmonic resonances and chaos in discontinuous dynamical systems has been reflected by amount of researchers in the past several years. Shaw and Holmes<sup>[1]</sup> analyzed a single-degree-of-freedom vibro-impact system by using the traditional approaches for demonstrating periodic-impact phenomena in the system. The results revealed all types of typical nonlinear behaviours: saddle-node and flip bifurcations, multiple coexisting attractors and chaos, etc. Nordmark<sup>[2]</sup> developed the discontinuity mapping method for investigating grazing dynamics and attendant bifurcations of the piecewise linear and vibro-impact systems. Ref.<sup>[3]</sup> focused on the grazing transitions from no impact to impact motion and investigated parameter space regions around the grazing bifurcations. Chin et al.<sup>[4]</sup> numerically generated three basic bifurcation scenarios such as reversed period adding cascade, hysteresis and period-M maximal orbit by using Nordmark map. Ref.<sup>[5]</sup> provides a comprehensive investigation of grazing motions in the dry-friction oscillator for a better understanding of the grazing mechanism of a discontinuous system. Experimental model of a base excited symmetrically piecewise linear oscillator was performed by Sin and Wiercigroch<sup>[6]</sup>. Luo<sup>[7,8]</sup> presented an idealized, piecewise linear system to model non-smooth vibration of gear transmission and studied the impact behaviour between the gear teeth. For example, in wheel-rail impacts of railway coaches<sup>[9]</sup>, Jeffcott rotor with bearing clearance<sup>[10]</sup>, gears transmissions<sup>[11]</sup>, small vibro-impact pile driver<sup>[12]</sup>, etc., impacting models have proved to be useful. Giusepponi et al.<sup>[13]</sup> demonstrated the chattering dynamics of an inelastic ball bouncing on the vibrating table. Ref.<sup>[14]</sup> studied the chattering sequence and correlative relationship between dynamic performance and system parameters of a two-degree-of-freedom periodically-forced system with a clearance.

A periodically-forced system with a rigid stop and clearance is established. The main purpose of the present study is to analyze the nonlinear characteristics of such system, including grazing and period doubling bifurcations, subharmonic motions, coexistence attractors, etc. A series of grazing bifurcations occurs with decreasing frequency so that the impact number  $p$  of  $p/1$  motions correspondingly increases one by one, a series of saddle-node bifurcations occur with increasing frequency so that the impact number  $p$  of  $p/1$  motions correspondingly decreases one by one and there exists frequency hysteresis and multiple coexistence attractors between  $p/1$  and  $(p+1)/1$  motions. In the low exciting frequency case, the impact number  $p$  of  $p/1$  motions becomes big enough and chattering-impact characteristics will be appearing. The transition law from  $1/1$  motion to chattering-impact motion is summarized explicitly.

MECHANICAL MODEL

The mechanical model of a two-degree-of freedom system with a rigid stop is shown in Figure 1. Displacements of the masses  $M_1$  and  $M_2$  are described by  $X_1$  and  $X_2$ , respectively. The masses  $M_1$  and  $M_2$  are connected by linear spring with stiffness  $K_1$  and linear viscous dashpot with damping constant  $C_1$ . The mass  $M_2$  is attached to the supporting base by the linear spring with stiffness  $K_2$  and linear viscous dashpot with damping constant  $C_2$ . The excitations on masses are harmonic with amplitudes  $P_1$  and  $P_2$ .  $\Omega$  is the excitation frequency, and  $\tau$  is the phase angle. The mass  $M_1$  begins to hit the rigid stop when the displacement  $X_1$  of mass  $M_1$  equals the clearance  $B$ , i.e.  $X_1(t) = B$ . The impact is described by a coefficient of restitution  $R$ .

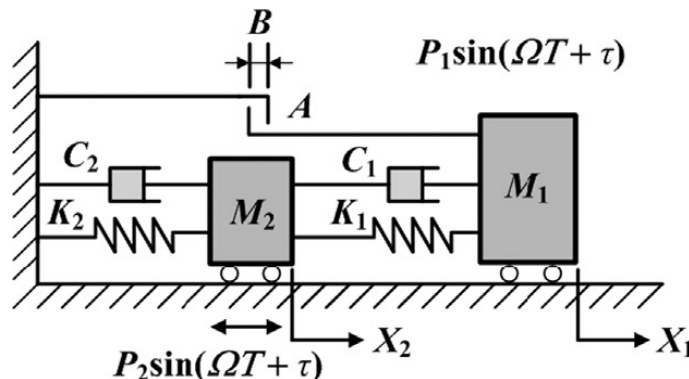


Figure 1 : Mechanical model of a periodic forced system with a rigid stop.

The motion processes of the system when the absolute value of displacement  $X_1$  is less than the clearance are considered. The condition of the periodic forced system, just immediately after impact, has become initial conditions in the subsequent process of the motion. The non-dimensional differential equations of motion are given by Equation (1).

$$\begin{bmatrix} 1 & 0 \\ 0 & \frac{\mu_m}{1-\mu_m} \end{bmatrix} \begin{Bmatrix} \ddot{x}_1 \\ \ddot{x}_2 \end{Bmatrix} + \begin{bmatrix} 2\zeta & -2\zeta \\ -2\zeta & \frac{2\zeta}{1-\mu_c} \end{bmatrix} \begin{Bmatrix} \dot{x}_1 \\ \dot{x}_2 \end{Bmatrix} + \begin{bmatrix} 1 & -1 \\ -1 & \frac{1}{1-\mu_k} \end{bmatrix} \begin{Bmatrix} x_1 \\ x_2 \end{Bmatrix} = \begin{Bmatrix} 1-f_{20} \\ f_{20} \end{Bmatrix} \sin(\omega t + \tau), \quad (x_1 < \delta) \quad (1)$$

A sudden change of velocity of the mass  $M_1$  occurs immediately after the impact, which is determined by Newton's hypothesis, i.e.,

$$\dot{x}_{1+} = -R\dot{x}_{1-}, \quad (x_1 = \delta) \quad (2)$$

where the subscript signs “-” and “+” denotethe states just before and after the impact, respectively.

The non-dimensional quantities of Equation (1) are given by

$$\begin{aligned} \mu_m &= \frac{M_2}{M_2 + M_1}, \quad \mu_k = \frac{K_2}{K_2 + K_1}, \quad \mu_c = \frac{C_2}{C_2 + C_1}, \quad \zeta = \frac{C_1}{2\sqrt{K_1 M_1}}, \quad f_{20} = \frac{P_2}{P_2 + P_1}, \quad \omega = \Omega \sqrt{\frac{M_1}{K_1}}, \\ \delta &= \frac{BK_1}{P_1 + P_2}, \quad t = T \sqrt{\frac{K_1}{M_1}}, \quad x_i = \frac{X_i K_1}{P_1 + P_2}, \quad i=1, 2. \end{aligned} \quad (3)$$

Periodic-impact motions of the system are described by the symbol  $p/n$ , where  $n$  denotes the number of excitation periods and  $p$  denotes the number of impacts with the rigid stop, during one impact motion period, respectively. In order to establish the Poincaré map of the periodic forced system, we chose the Poincaré section:  $\sigma_p = \{(x_1, \dot{x}_1, x_2, \dot{x}_2, t) \in R^4 \times S, x_1 = \delta, \dot{x}_1 = \dot{x}_{1-}\}$ . The disturbed map of  $1/n$  motion is represented briefly by

$$X_0^{(i+1)} = \tilde{f}(v, X_0^{(i)}) \quad (4)$$

where  $X \in R^4$ ,  $v$  are real parameters,  $v \in R^m$ ,  $X_0^{(i+1)} = X^* + \Delta X_0^{(i+1)}$ ,  $X_0^{(i)} = X^* + \Delta X_0^{(i)}$ ,  $X^* = (\tau_0, x_{20}, \dot{x}_{1-}, \dot{x}_{20})^T$  is a fixed point in the Poincaré section  $\sigma_p$ , its disturbed vectors is represented by  $\Delta X_0^{(i)} = (\Delta \tau^{(i)}, \Delta x_2^{(i)}, \Delta \dot{x}_{1-}^{(i)}, \Delta \dot{x}_2^{(i)})^T$ ,  $\Delta X_0^{(i+1)} = (\Delta \tau^{(i+1)}, \Delta x_2^{(i+1)}, \Delta \dot{x}_{1-}^{(i+1)}, \Delta \dot{x}_2^{(i+1)})^T$ , respectively.

The Poincaré section  $\sigma_n = \{(x_1, \dot{x}_1, x_2, \dot{x}_2, t) \in R^4 \times S, x_1 = x_{1p}, \text{mod}(t = 2\pi/\omega)\}$  is also considered to construct the other map. Consequently, the number  $p$  and  $n$  of  $p/n$  motion can be determined easily by the Poincaré map  $\sigma_p$  and  $\sigma_n$  respectively.

## CHARACTERISTIC AND TRANSITION LAW OF CHATTERING-IMPACT MOTIONS

The existence and stability of  $p/1$  and chattering-impact motions is analyzed explicitly. Grazing bifurcations at the boundary of  $p/1$  motions with decreasing frequency are considered. Particularly, the grazing bifurcation series from  $4/1$  orbit to  $5/1$  orbit is interrupted and there exists different kinds of periodic motions such as  $8/2$ ,  $7/2$ ,  $10/3$ ,  $13/4$ , etc.

Taking dimensionless parameters (1):  $\mu_m = 0.67$ ,  $\mu_k = 0.84$ ,  $\mu_c = 0.80$ ,  $\zeta = 0.10$ ,  $f_{20} = 0.00$ ,  $\delta = 0.77$  and  $R = 0.80$ , we analyze the nonlinear dynamic performances of the two-degree-freedom periodically forced system with a rigid stop. The global bifurcations of the rigid stop system, in the form of projected Poincaré section  $\sigma_p$ , is shown for  $\omega$  varying in the range  $[0.2, 0.8]$ , see Figure 2. The sign  $G_{p/1}$  denotes the grazing bifurcation boundary of  $p/1$  to  $(p+1)/1$  periodic orbit. Figure 3 is the detail local bifurcations of Figure 2. It is shown that the system exhibits stable  $1/1$  motion with  $\omega \in [0.6646, 0.8]$ . When the frequency  $\omega$  is decreased to  $\omega_c = 0.6646$ , the mass  $M_1$  begins to touch the rigid stop with zero velocity and the grazing bifurcation occurs, the  $1/1$  motion has changed its stability so that the impact number  $p$  increases one and the  $2/1$  impact motion is born. The stable  $2/1$  motion exists in the frequency interval  $\omega \in (0.4576, 0.6646)$ . As  $\omega$  passes through  $\omega_c = 0.4576$  decreasingly, grazing bifurcation associated with the motion occurs and the stable  $3/1$  motion takes place after the grazing bifurcation immediately. Figure 4 shows the  $1/1$  motion with grazing contact for  $\omega_c = 0.6646$  and Figure 5 shows the  $2/1$  motion with grazing contact for  $\omega_c = 0.4576$ . From Figure 3, several frequency windows of chaos and periodic motion exist analogously, such as  $13/4$ ,  $10/3$ ,  $7/2$ ,  $8/2$ , etc. For example, the  $10/3$  motion turns into chaos from grazing bifurcation

with decreasing frequency and then a sequence of inverse period-doubling bifurcations appears. The 7/2 motion fall into chaos and then 4/1 fundamental motion is born via the inverse period-doubling bifurcations.

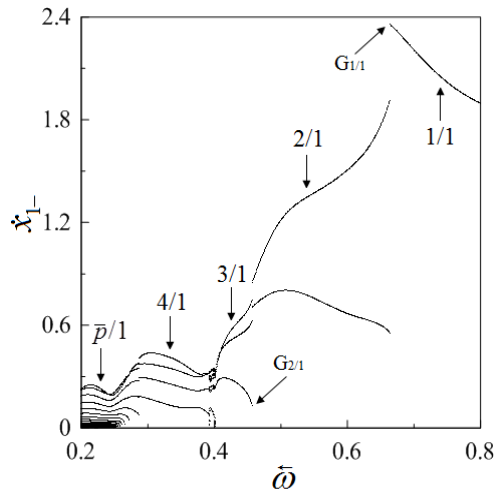


Figure 2 : Bifurcation diagram with decreasing frequency  $\omega$  .

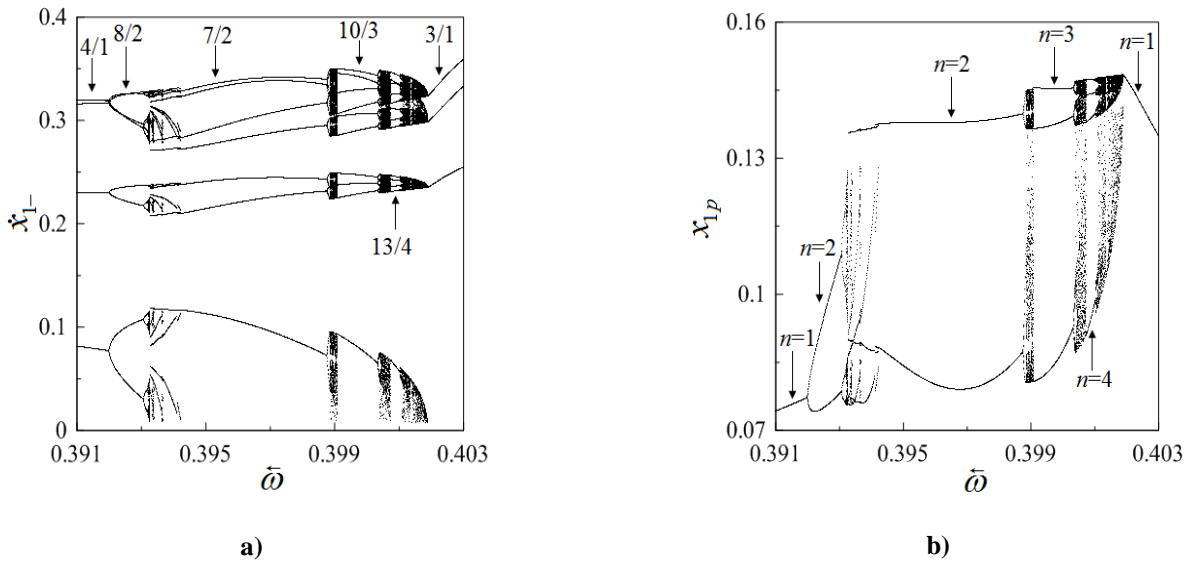


Figure 3 : Details of Figure 2: a) Bifurcation diagram of Poincaré map  $\sigma_p$ , b) Bifurcation diagram of Poincaré map  $\sigma_n$  .

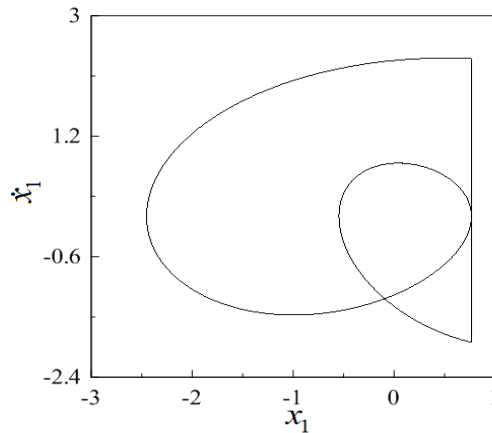


Figure 4 : Phase portrait of 1/1 motion with grazing contact,  $\omega=0.6646$ .

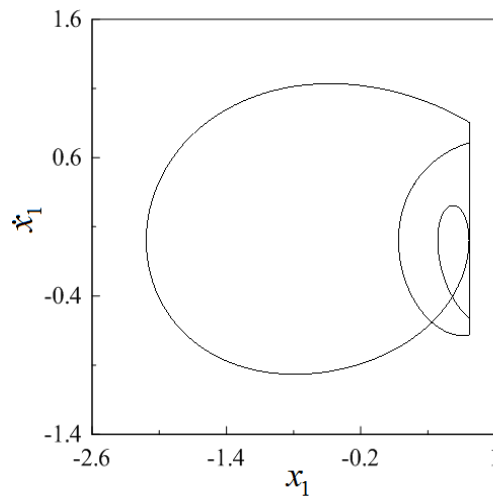


Figure 5 : Phase portrait of 2/1 motion with grazing contact,  $\omega=0.4576$ .

A series of grazing bifurcations occurs with decreasing the frequency  $\omega$  so that the number  $p$  of impacts of  $p/1$  motions increases one by one. As  $p$  becomes big enough, the  $p/1$  motion exhibits chattering-impact characteristics. The lower the frequency  $\omega$  is, the more the impact number  $p$  is. Consequently, the transition law from 1/1 motion to chattering-impact motion is summarized as follows

$$\omega \downarrow: \bar{p}/1 \xleftarrow{\text{S Bif}} \dots \xleftarrow{\text{G Bif}} \tilde{p}/1 \xleftarrow{\text{G Bif}} \dots \xleftarrow{\text{G Bif}} (p+1)/1 \xleftarrow{\text{G Bif}} p/1 \xleftarrow{\text{G Bif}} \dots \xleftarrow{\text{G Bif}} 2/1 \xleftarrow{\text{G Bif}} 1/1. \tag{5}$$

where the symbol  $\bar{p}/1$  denote the chatting-impact motion with sticking and  $\tilde{p}/1$  represent the chattering-impact motion without sticking, S Bif and G Bif represent sliding and grazing bifurcations, respectively. Figure 6 shows the time series of 3/1, 5/1 and chattering-impact motion.

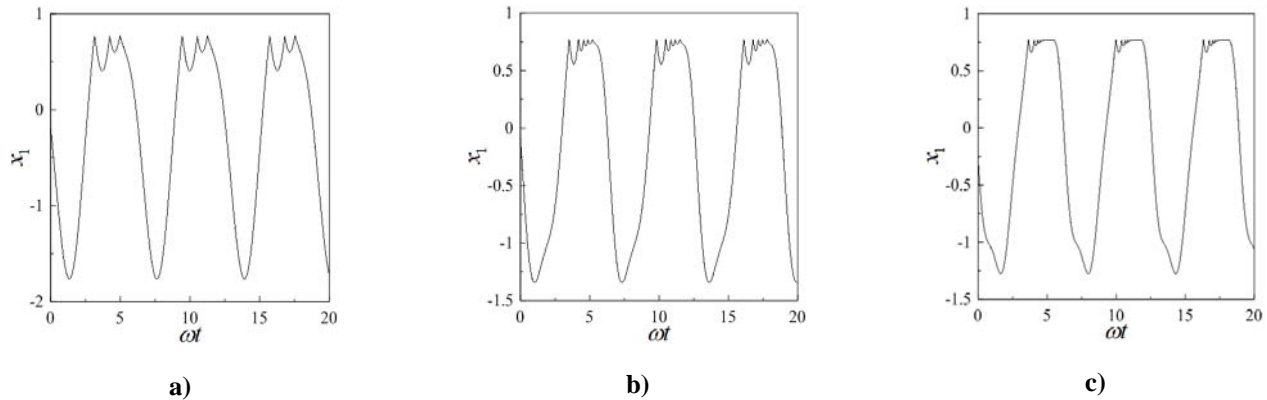


Figure 6 : Time series of: a) 3/1 motion,  $\omega=0.42$ , b) 5/1 motion,  $\omega=0.28$ , c) chattering-impact motion,  $\omega=0.22$ .

SUBHARMONIC MOTIONS

Taking dimensionless parameters (2):  $\mu_m = 0.67$ ,  $\mu_k = 0.84$ ,  $\mu_c = 0.80$ ,  $\zeta = 0.10$ ,  $f_{20} = 0.00$ ,  $\omega = 0.82$  and  $R = 0.80$ , we analyze the nonlinear dynamic performances of the rigid stop system with decreasing the clearance  $\delta$ . The global bifurcations of the rigid stop system, in the form of projected Poincaré section  $\sigma_p$  and  $\sigma_n$ , is shown for  $\delta$  varying in the range [2.0,5.6], see Figure 7.

The  $1/n$  subharmonic motions ( $n=1, 2, 3, 4, 5$ ) are easily demonstrated by Figure 7. This is the period adding cascade referred in Ref.<sup>[4]</sup>. The chaos motions appears via the grazing bifurcation of  $1/n$  motion and the  $1/(n-1)$  subharmonic motion occurs through the reversed period doubling bifurcation from chaos with increasing the clearance  $\delta$ . However, we can note that existence windows of  $2/2n$  motions ( $n=1, 2, 3, 4, 5$ ) are too small to be observed. In Figure 8, the phase portrait 1/3orbit with grazing contact is shown at  $\delta = 4.45$ . The chaos via the grazing bifurcation of 1/3 motion is depicted by the phase portrait shown in Figure 9.

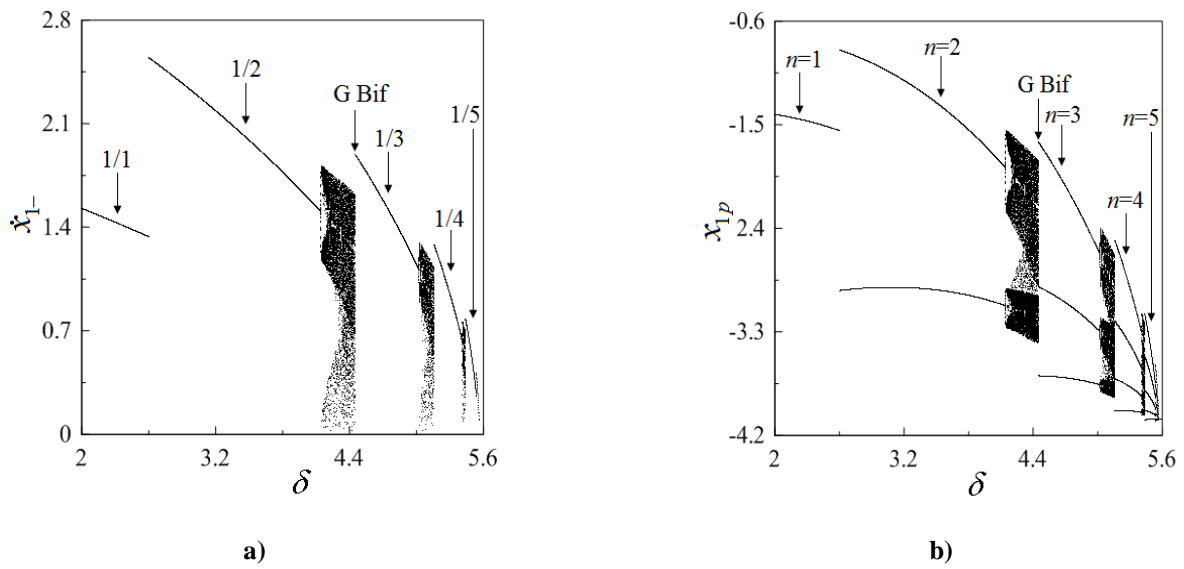


Figure 7 : Bifurcation diagrams with decreasing clearance  $\delta$  : a) Diagram of Poincaré map  $\sigma_p$ , b) Diagram of Poincaré map  $\sigma_n$

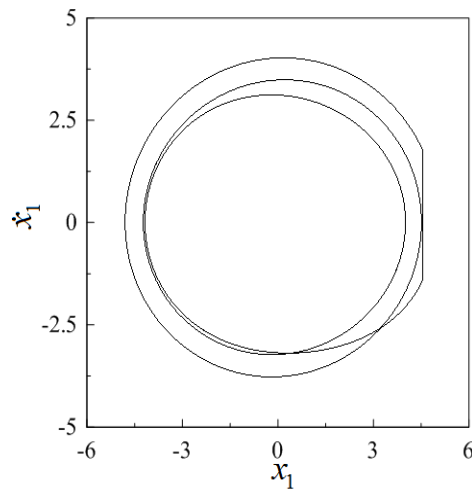


Figure 8 : Phase portrait of 1/3 subharmonic motion with grazing contact,  $\delta = 4.45$ .

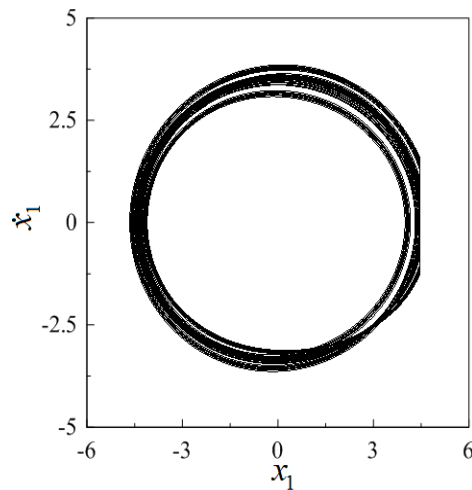


Figure 9 : Phase portrait of chaos,  $\delta = 4.449$ .

COEXISTENCE ATTRACTORS

Taking dimensionless parameters (1), the global bifurcation diagrams of the rigid stop system, in the form of projected Poincaré section  $\sigma_p$ , are shown with increasing or decreasing frequency  $\omega$  varying in the range [0.2,0.8], as seen in Figure 10. The sign  $SN_{p/1}$  and  $FH_{(p-1)/1}$  denotes the saddle-node bifurcation boundary and frequency hysteresis range of  $p/1$  orbit to  $(p-1)/1$  orbit. For the sake of exhibition, the global bifurcation diagrams with increasing or decreasing frequency  $\omega$  were plotted in the same diagram.

Saddle-node bifurcations at the boundary of  $p/1$  motions with increasing frequency are considered. On the boundary  $SN_{p/1}$ , one of impacts of the motion disappears and  $(p-1)/1$  motion occurs after a jump transition. A narrower frequency hysteresis range exists between grazing boundary of  $p/1$  motion and saddle-node bifurcation boundary of  $(p+1)/1$  motion, as seen in Figure 10. There coexist both stable  $p/1$  and  $(p+1)/1$  motions in the dependence on different initial conditions or on the way of the system parameters change in the frequency hysteresis ranges. Figure 11 shows the coexistence periodic orbits of 1/1 motion and 2/1 motion in the frequency hysteresis range  $FH_{1/1}$  at  $\omega=0.67$ . Figure 12 shows the coexistence periodic orbits of 2/1 motion and 3/1 motion in another frequency hysteresis range  $FH_{2/1}$  at  $\omega=0.4577$ .

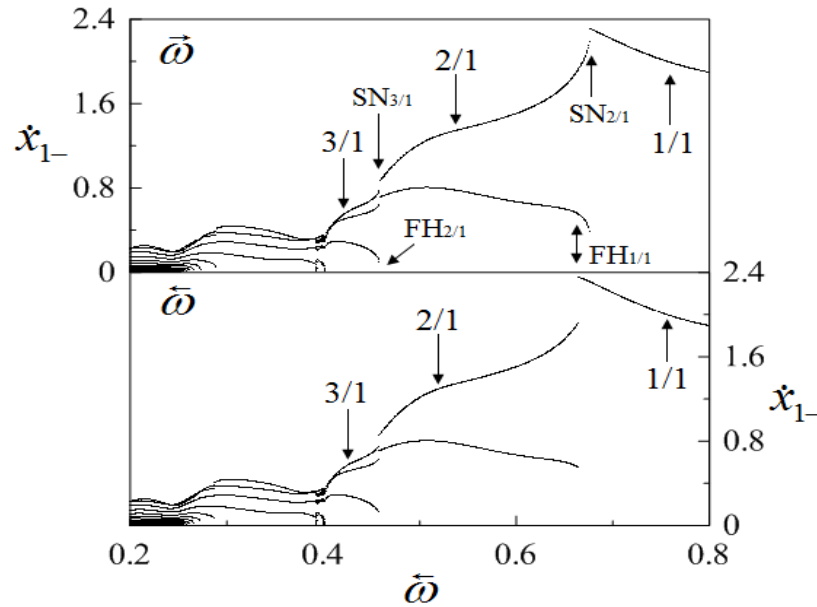


Figure 10 : Diagram of frequency hysteresis range of the saddle-node bifurcations.

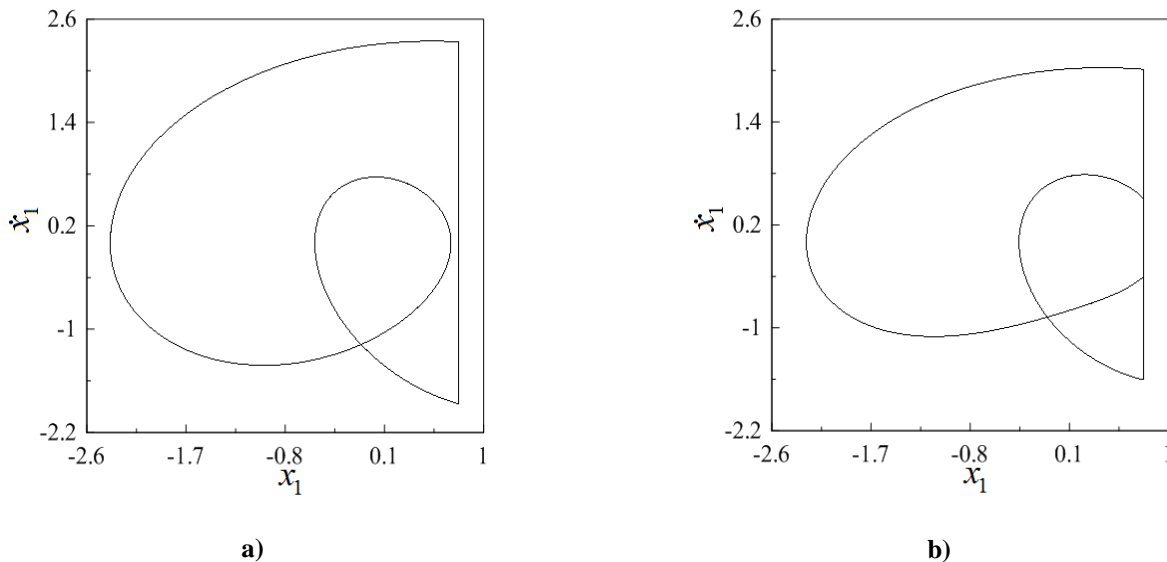
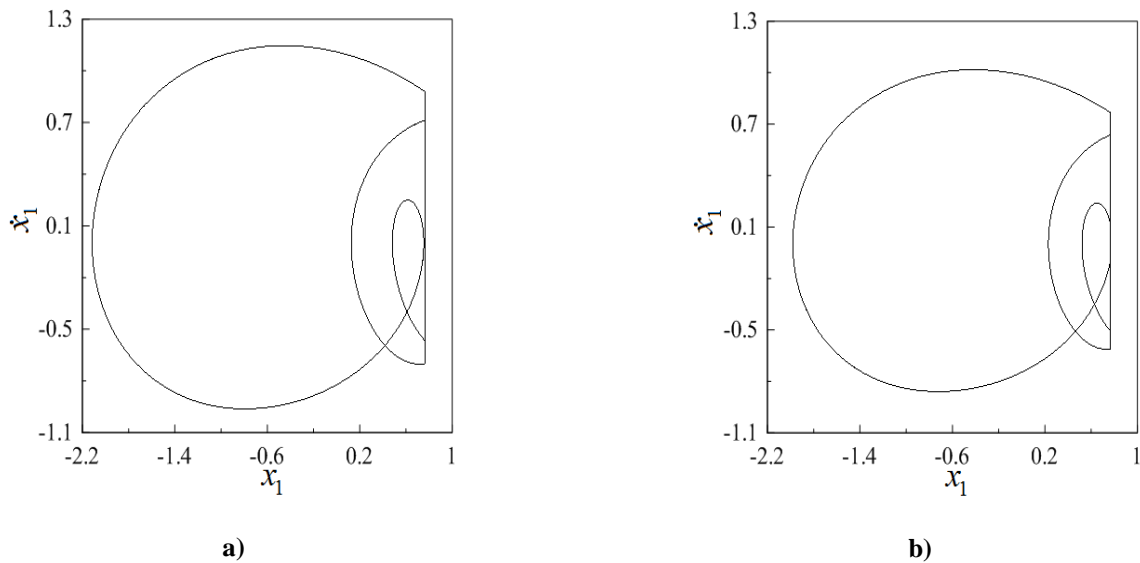


Figure 11 : Phase portraits of coexistence attractors,  $\omega=0.67$ : a) Phase portrait of 1/1 motion, b) Phase portrait of 2/1 motion.



**Figure 12 : Phase portraits of coexistence attractors,  $\omega=0.4577$ : a) Phase portrait of 2/1 motion, b) Phase portrait of 3/1 motion.**

### CONCLUSIONS

In this paper, the mechanical model and two different Poincaré maps of the period-forced system with a rigid stop were established. The nonlinear characteristics of the system were analyzed with special attention to grazing bifurcation, saddle-node bifurcation, subharmonic motions, chattering-impact motions and coexistence attractors, etc.

(1). A series of grazing bifurcations occur with decreasing frequency so that the impact number  $p$  of  $p/1$  motions correspondingly increases one by one. In the low exciting frequency case, the impact number  $p$  of  $p/1$  motions becomes big enough and chattering-impact characteristics will be appearing. The transition law from 1/1 motion to chattering-impact motion is summarized explicitly.

(2). Particularly, several  $p/1$  fundamental motion sequence with decreasing frequency is interrupted by the grazing bifurcations, chaos and reverse period-doubling bifurcations, there exists different kinds of periodic motions in the specific frequency windows, such as 8/2, 7/2, 10/3, 13/4, etc.

(3). A series of saddle-node bifurcations occur with increasing frequency so that the impact number  $p$  of  $p/1$  motions correspondingly decreases one by one and there exist frequency hysteresis ranges and multiple coexistence attractors between  $p/1$  and  $(p+1)/1$  motions.

(4). The subharmonic motions and period adding cascade was numerically generated by choosing special system parameters.

### ACKNOWLEDGEMENT

The authors gratefully acknowledge the support by Natural Science Foundation of Gansu Province (145RJZA056), Youth scientific funds of the Lanzhou Jiaotong University (2013024) and Pre-research funds of Jinchuan Group CO., LTD. (420032).

### REFERENCES

- [1] S.W.Shaw, P.J.Holmes; A periodically forced piecewise linear oscillator, in *Journal of Sound and Vibration*, **90(1)**, 129-155 (1983).
- [2] A.B.Nordmark; Non-periodic motion caused by grazing incidence in an impact oscillator, in *Journal of Sound and Vibration*, **145(2)**, 279-197 (1991).
- [3] S.L.T.De Souza, M.Wiercigroch; Suppressing grazing chaos in impacting system by structural nonlinearity, in *Chaos, Solitons and Fractals*, **38**, 864-869 (2008).
- [4] W.Chin, E.Ott, H.E.Nusse, C.Grebogi; Grazing bifurcations in impact oscillators, in *Physical Review E*, **50**, 4427-4444 (1994).
- [5] A.C.J.Luo, B.C.Gegg; Grazing phenomena in a periodically forced, friction-induced, linear oscillator, in *Communications in Nonlinear Science and Numerical Simulation*, **11**, 777-802 (2006).
- [6] M.Wiercigroch, V.T.W.Sin; Experimental study of a symmetrical piecewise base-excited oscillator, in *ASME Journal of Applied Mechanics*, **65(3)**, 657-663 (1998).
- [7] A.C.J.Luo, D.O'Connor; Periodic motions and chaos with impacting chatter and stick in a gear transmission system, in *International Journal of Bifurcation and Chaos*, **19(6)**, 1975-1994 (2009).



- [8] A.C.J.Luo, D.O'Connor; Mechanism of impacting chatter with stick in a gear transmission system, *International Journal of Bifurcation and Chaos*, **19(6)**, 2093-2105 (2009).
- [9] G.W.Luo, J.N.Yu, H.M.Yao, J.H.Xie; Periodic-impact motions and bifurcations of the vibratory system with a clearance, in *Chinese Journal of Mechanical Engineering*, **42**, 88-94 (2006).
- [10] E.V.Karpenko, M.Wiercigroch, E.E.Pavlovskaja, R.D.Neilson; Experimental verification of Jeffcott rotor model with preloaded snubber ring, in *Journal of Sound and Vibration*, **298(4-5)**, 907-917 (2006).
- [11] A.Al-Shyyab, A.Kahraman; Non-linear dynamic analysis of a multi-mesh gear train using multi-term harmonic balance method: Sub-harmonic motions, in *Journal of Sound and Vibration*, **279(1-2)**, 417-451 (2005).
- [12] G.W.Luo, H.M.Yao; Dynamics of a small vibro-impact pile driver, in *Nonlinear Analysis: Real World Applications*, **9(4)**, 1361-1377 (2008).
- [13] S.Giusepponi, F.Marchesoni, M.Borromeo; Randomness in the bouncing ball dynamics, in *Physica A*, **351(1)**, 142-158 (2005).
- [14] G.W.Luo, X.H.Lv, Y.Q.Shi; Vibro-impact dynamics of a two-degree-of freedom periodically-forced system with a clearance: Diversity and parameter matching of periodic-impact motions, in *International Journal of Non-Linear Mechanics*, **65**, 173-195 (2014).